PAPER

Check for updates

Heterologous expression of the cryptic *mdk* gene cluster and structural revision of maduralactomycin A†

Jan W. Schwitalla, [ID] [ab] Ngoc-Thao-Hien Le,[c] Soohyun Um,[d] Felix Schalk, [ID] [a] Mark Brönstrup, [ID] [e] Martin Baunach[f] and Christine Beemelmanns [ID] *[abg]

After conducting an *in silico* analysis of the cryptic *mdk* cluster region and performing transcriptomic studies, an integrative *Streptomyces* BAC Vector containing the *mdk* gene sequence was constructed. The heterologous expression of the *mdk* cluster in *Streptomyces albus* J1074 resulted in the production of the angucyclic product, seongomycin, which allowed for the assesment of its antibacterial, antiproliferative, and antiviral activities. Heterologous production was further confirmed by targeted knock-out experiments involving key regulators of the biosynthetic pathways. We were further able to revise the core structure of maduralactomycin A, using a computational approach.

1. Introduction

In recent years, actinobacteria associated with insects have garnered significant attention from natural product chemists worldwide.[1] This is owing to their frequently remarkable biosynthetic capacity, and their role in host defense mechanisms through the secretion of bioactive compounds.[2,3] By combining ecology-based natural product discovery techniques with analytical dereplication strategies, scientists have unveiled a multitude of structurally distinct and protective metabolites.[4] As part of our ecology-guided natural product discovery efforts, the bacterial symbiont of fungus-growing termites, named *Actinomadura rubteroloni* (*Actinomadura* sp. RB29),[5,6] attracted our attention due to its antagonistic effect against parasitic co-isolated fungi of *Macrotermes natalensis*. MS-guided chemical analyses led to the

[a]Chemical Biology of Microbe-Host Interactions, Hans-Knöll Institute (HKI), Beutenbergstraße 11a, 07745 Jena, Germany

[b]Helmholtz Institute for Pharmaceutical Research Saarland (HIPS), Helmholtz Centre for Infection Research (HZI), Campus E8, 66123, Saarbrücken, Germany. E-mail: christine.beemelmanns@helmholtz-hips.de

[c]Department of Pharmaceutical Sciences, Natural Products and Food Research and Analysis (NatuRA), University of Antwerp, Universiteitsplein 1, B-2610 Antwerp, Belgium

[d]College of Pharmacy, Yonsei Institute of Pharmaceutical Sciences, Yonsei University, Incheon, 21983, South Korea

[e]Department of Chemical Biology, Helmholtz Centre for Infection Research, Inhoffenstrasse 7, D-38124 Braunschweig, Germany

[f]Institute of Pharmaceutical Biology, University of Bonn, Nussallee 6, 53115 Bonn, Germany

[g]Saarland University, 66123, Saarbrücken, Germany

† Electronic supplementary information (ESI) available: The datasets supporting this article have been uploaded as part of the ESI and contains details for chemical procedures, 1D and 2D NMR of described compounds, as well as HRMS data and bioassay data. See DOI: https://doi.org/10.1039/d3ra05931f
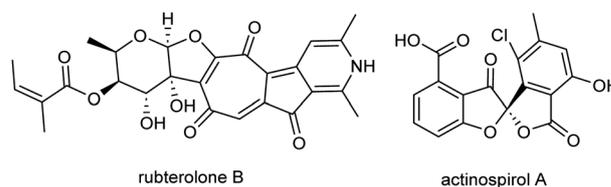
Fig. 1 Chemical structures of rubterolone B and actinospirol A.

isolation of antifungal lanthipeptide rubrominins, the polyketide-derived rubterolones,[7–10] and the halogenated angucyclic maduralactomycins and spirocyclic actinospirols (Fig. 1).[11] In an initial genome-mining endeavour, a potential type II polyketide synthase (PKS) gene cluster region, designated as *mdk* and spanning approximately 36 kbp, was identified. Subsequent RT-PCR analysis revealed that transcription of the *mdk* biosynthetic gene cluster (BGC) occurred exclusively when *A. rubteroloni* was cultivated from spores in modified ISP5 medium; otherwise, it remained dormant.

In this study, we tested if the proposed *mdk* BGC is indeed responsible for the production of angucyclic natural products by heterologous expression. Findings of this study enabled us to isolate the heterologously produced angucyclic product seongomycin and stimulated research on its biological origin. Results of our biosynthetic studies also stimulated the application of computational chemical shift prediction tools, and results of these studies allowed us to revise the planar structure of maduralactomycin A.

2. Experimental

2.1 Materials and methods

2.1.1 Chemicals. All media and ingredients and chemicals were purchased as follows: methanol (Th. Geyer, Renningen);

water for analytical and preparative HPLC (Millipore, Germany); formic acid (Carl Roth, Germany); acetonitrile (Th. Geyer, Renningen); DMSO (Carl Roth, Germany); media ingredients (Carl Roth, Germany).

2.1.2 Strains and culture conditions. *Actinomadura* sp. RB29 was sub-cultured in 50 mL ISP2 broth for seven days at 30 °C and 120 rpm (Tables S1–S3†). *E. coli* was cultivated in Luria–Bertani (LB) broth for cryopreservation, bacteria were stored in 25% glycerol at −80 °C. Culture media were autoclaved at 121 °C for 20 min. For selection of transformants and ex-conjugants, media were supplemented with antibiotics (depending on the purpose): apramycin, chloramphenicol, kanamycin, spectinomycin or nalidixic acid.

2.1.3 General procedure for DNA amplification. Cells were harvested by centrifugation from a bacterial culture (1 mL, 5000 rpm, 10 min, room temperature). DNA isolation was performed with the GeneJET Genomic DNA Purification Kit (Thermo Scientific, Waltham, USA) according to the manufactures protocol with minor adjustments: cell wall lysis was performed for one hour instead of 30 min, the protein lysis step was prolonged to 40 min and the RNA lysis step was set to 15 min. The concentration of the DNA was determined *via* NanoDrop Lite (Thermo Scientific, Waltham, USA). Isolated DNA was immediately frozen and stored at −20 °C. The Zymoclean Gel DNA Recovery Kit was used for isolation of nucleic acids from agarose gel according to the manufacturer's protocol and DNA sequenced with Eurofins Genomics.

2.1.4 RNA sequencing. *Actinomadura* sp. RB29 spores were used for inoculation[11] and *Actinomadura* sp. RB29 was grown for seven days on ISP2 (non-producing conditions) and ISP5 media (producing conditions).[11] Cells were harvested from agar plates (10 g) and flash frozen in liquid nitrogen. RNA extraction and RNA sequencing was performed by Novogen Sequencing Europe and data was visualized using Rstudio.

2.1.5 Gene cluster comparison and phylogenetic analysis. To evaluate the distribution of the *mdk* sequence in bacterial genomes and to compare the relative abundance, homology searches were conducted using antiSMASH V6.0 (ref. 12) and a cblaster[13] search. Results of these searches were visualized using the clinker tool.[14] For phylogenetic analysis, respective amino acid sequences were aligned using ClustalW and the phylogenetic tree was built with *via* the NaPDoS2. The phylogenetic trees were visualized using iTOL (Fig. S1–S4†).

2.1.6 Cloning of the *mdk* gene cluster. For vector construction, isolated gDNA *Actinomadura* sp. RB29 was cut with Cas9 using guide RNA sequences and monitored by qPCR assays using primers designed for both the left and right cut sites of the cluster (Varigen Biosciences, now Terra Bioforge). After verification of digestion efficiency, DNA assembly of the genomic preparation was performed to linearized pDualP vector containing overlap regions specific to the target fragment. The DNA assembly reaction was transformed to *E. coli* BacOpt2.0 from which colonies were recovered carrying the *mdk* containing pDualP vector (named SPIRO). Colonies were assayed *via* colony PCR using primers for both the left and right cloning junctions and sequences confirmed by Sanger sequencing. Clones for the construct were restriction digested separately

and compared to a simulated digest to confirm the insertion of the whole BGC into the vector backbone.

Cloning of the *mdk* gene cluster into the heterologous host was performed based on a conjugation protocol described by Kieser *et al.*,[15] which was modified for tri-parental conjugation. Briefly, an overnight pre-culture of *E. coli* carrying the *mdk* containing pDualP vector and *E. coli* HB101 : prK2013 (carrying the helper plasmid for conjugational transfer) was inoculated and grown to an OD of approx. 0.4 at 30 °C. These cells were washed two times with LB media and cooled to 0 °C on ice. Next, SPIRO BGC containing *E. coli* were mixed with *E. coli* HB101 : prK2013 in a ratio of 1 : 1. Heat shocked spores from *S. albus* J1074 were added in a ratio of 1 : 1, inverted and the *Streptomyces*/*E. coli* mixture was plated on MS media with 10 mM MgCl$_2$. After 16–20 h of growth at 30 °C, plates were overlaid first with 1 mL of an antibiotic solution containing spectinomycin (5 mg mL^{-1}) and nalidixic acid (0.5 mg mL^{-1}). For selection of strains carrying the modified plasmid, plates were also overlaid with 1 mL of an antibiotic solution containing apramycin (1.25 mg mL^{-1}) and nalidixic acid (0.5 mg mL^{-1}). After one week of growth exconjugants were selected and grown on MS-agar (20 g per L agar, 20 g per L mannitol, 20 g per L soy flour, supplemented with apramycin (50 μg mL^{-1}) and nalidixic acid (25 μg mL^{-1})). Positive clones were identified and verified by gene amplification and sequencing (Table S3 and Fig. S5–S8†).

2.1.7 Genetic manipulations. Genetic manipulations were performed using the established λ Red system for *Streptomyces* species.[16]. Briefly, a knockout cassette was generated consisting of a spectinomycin resistance with homologous ends to the gene targeted for knockout. This construct was electroporated into arabinose induced *E. coli* BW25113/piJ790 harboring the λ Red plasmid piJ790 and the SPIRO plasmid, which was electroporated earlier. These induced cells were grown on selective LB media containing the antibiotics apramycin and spectinomycin (each 50 μg mL^{-1}). Mutated plasmids were isolated and transferred to the *Streptomycete* host *via* conjugation. Presence of the knockout plasmid inside the heterologous host was verified by PCR using diagnostic primers and sequencing (Tables S4, S5 and Fig. S5–S8†).

2.1.8 Extraction of metabolites from culture supernatants. A three-day-old seed culture (5 mL) of the respective strain was added to baffled flasks (500 mL) containing 100 mL modified DNPM media supplemented with apramycin (20 μg mL^{-1}). Cultures were incubated at 140 rpm and 30 °C. After one day of growth, the inducer compounds ε-caprolactam (up to 0.1%) and/or oxytetracyclin (2.5 μM) were added to induce gene expression. Bacterial cultures were harvested after 3, 5 and 7 days of growth and cells separated by centrifugation (45 min, 10 000 rpm, 4 °C). The collected supernatant was adjusted to 5% MeOH and subjected to solid phase extraction (SPE) using equilibrated octadecyl-modified silica gel (6 mL/1 g, C$_{18}$-modified silica gel at 5% MeOH in dH$_2$O). After loading the column using 50 mL of bacterial supernatant, the columns were washed with two CV 5% MeOH and metabolites were first eluted with three CV 10% MeOH and three CV of increasing MeOH concentration (30%, 60%, 100%). Obtained eluates were

combined and concentrated under reduced pressure. The resulting organic extracts were re-dissolved in MeOH (50%) at a concentration of 50 µg mL^{-1} for subsequent HRMS/MS analysis.

LC-ESI-HRMS based metabolomics was performed on a Dionex Ultimate3000 system equipped with a Luna Omega C18 column (100 × 2.1 mm, particle size 1.6 µm, pore diameter 100 Å, Phenomenex) coupled with a Q-Exactive Plus mass spectrometer (Thermo Scientific) equipped with an electrospray ion (HESI) source. The column oven temperature was set to 40 °C; scan range of full MS was set to m/z 180 to 2000 with a resolution of 70 000 and AGC target 3 × 10^6 and maximum IT 100 ms under positive mode with centroid data type. MS^2 analysis was performed as top10 experiments (positive mode) with a resolution of 17 500 and AGC target 1 × 10^5 and maximum IT 50 ms and a normalized collision energy (NCE) of 28. The spray voltage (+) was set to 4000 volt, and (−) was set to 3300 volt. The capillary temperature (±) was set to 340 °C and probe heater temperature (±) was set to 200 °C. The sheath gas flow (±) was set to 35 L min^{-1} and Aux gas flow (±) to 5 L min^{-1}. Max spray current (+) and (−) was set to 100 volt. S-Lens RF level was set to 50.

2.1.9 Network-based metabolomic analysis of culture extracts. A molecular network of obtained HRMS/MS data was created using the online workflow on the GNPS website (http://gnps.ucsd.edu).[17] The data was filtered by removing all MS/MS fragment ions within ±17 Da of the precursor m/z. MS/MS spectra were window filtered by choosing only the top 6 fragment ions in the ±50 Da window throughout the spectrum. The precursor ion mass tolerance was set to 0.02 Da and a MS/MS fragment ion tolerance of 0.02 Da. A network was created where edges were filtered to have a cosine score above 0.6 and more than 4–6 matched peaks (depending on the experiment). Further, edges between two nodes were kept in the network if and only if each of the nodes appeared in each other's respective top 10 most similar nodes. Finally, the maximum size of a molecular family was set to 100, and the lowest scoring edges were removed from molecular families until the molecular family size was below this threshold. The spectra in the network were then searched against GNPS' spectral libraries.[18] The library spectra were filtered in the same manner as the input data. All matches kept between network spectra and library spectra were required to have a score above 0.7 and at least 6 matched peaks. Data was visualized using Cytoscape 3.8.0 software (Tables S6–S8 and Fig. S9–S19†).

2.1.10 Isolation of seongomycin. A seven-day-old culture of SAS116 α (400 mL, DNPM media) was induced with ε-caprolactam, and the culture was harvested after incubation by centrifugation as described above. The culture supernatant was adjusted to 5% MeOH and extracted using an activated SPE column (5 g column, C$_{18}$-silica gel). Elution was done using four CV 10% MeOH, 4 CV of 30% MeOH and four CV 100% MeOH. Fractions 10% and 30% MeOH containing seongomycin were concentrated under reduced pressure and re-dissolved in MeOH (3 mg mL^{-1}) for subsequent preparative HPLC purification. The vanquish preparative HPLC system (Thermo Scientific) equipped with Chromeleon 7.3.2 software and a Luna C18

(250 × 10 mm, 100 Å) column was used for purification (Fig. S20†). A gradient with a constant flow rate of 20 mL min^{-1} consisting of buffer A: CH$_3$CN + 0.1% B: H$_2$O + 0.1% FA was applied as follows: 0–5 min, A: 10%; 5–45 min A: 5–90%; 45–50 min, A: 95%; 55–60 min, A: 10%. The fraction containing seongomycin was collected and dried under reduced pressure. NMR measurements were performed on a Bruker AVANCE III 500 MHz and 600 MHz spectrometer, equipped with a Bruker Cryoplatform. The chemical shifts are reported in parts per million (ppm) relative to the solvent residual peak of DMSO-d_6 (^{1}H: 2.50 ppm, quintet; ^{13}C: 39.52 ppm, heptet) (Tables S9, S10 and Fig. S21–S32†).

2.1.11 Computational calculations of chemical shifts. Monte Carlo conformational search was performed by PCMODEL (version 10.0) using MMFF94 force field, which applies 8 and 7 kcal mol^{-1} energy windows for two consecutive conformational search cycles. Afterwards, for chemical shift calculations, all resulting conformers were subjected to geometry optimization using B3LYP/6-31+G(d,p) level of theory in gasphase, and shielding tensors were then computed at mPW1PW91/6-311+G(2d,p) level of theory with polarizable continuum model (PCM). Geometry optimization, frequencies and shielding tensor calculation were carried out with Gaussian16 software. Boltzmann distributions were estimated from the B3LYP/6-31+G(d,p) level of theory using the sum of electronic and thermal free energies at 298.15 K. Only conformers with energies within 2.5 kcal mol^{-1} from the global minimum were submitted to the GIAO calculation of shielding tensors. After dereplication, resulting isotropic shielding values were scaled using the following slopes and intercepts (for ^{1}H nuclei, slope = −1.0936 and intercept = 31.8018; for ^{13}C nuclei, slope = −1.0533 and intercept = 186.5242) (Tables S11–S21 and Fig. S33–S34†).[19,20]

2.1.12 Antiproliferative activity assays. Cells and culture conditions for cytological assays: cells were grown in the appropriate cell culture medium at 37 °C in 5% CO$_2$ in highdensity polyethylene flasks. Test substances were dissolved in DMSO before being diluted in cell culture medium. The adherent cells were harvested at the logarithmic growth phase after soft trypsinization using 0.25% trypsin in PBS containing 0.02% EDTA. For each experiment, approximately 10 000 cells were seeded with 0.1 mL culture medium per well of the 96-well microplates. To test the antiproliferative effect of natural products, the cells were incubated for 72 hours in plates prepared with control and different dilutions of test substances. The GI50 values were defined as being where the inhibition of proliferation is 50% compared to untreated control (Tables S23–S25 and Fig. S35–S36†).

3. Results and discussion

3.1 Gene cluster analysis

We first reanalysed the gene cluster region *mdk*, which contains about 21 genes including the core PKS-encoding genes (*mdk*A, *mdk*B, *mdk*C, *mdk*D, *mdk*E, *mdk*I), five genes coding for oxidative enzymes (*mdk*G, *mdk*OR, *mdk*O1, *mdk*O2, *mdk*O3), and one halogenase (*mdk*H) (Fig. 2 and S1†), which were flanked by at
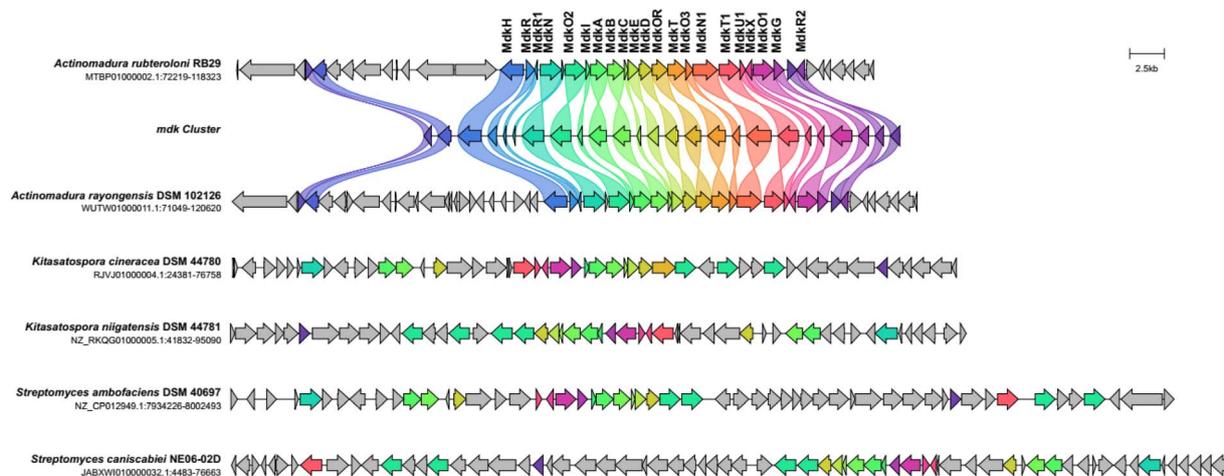
Fig. 2 Cblaster analysis using the *mdk* gene cluster sequence as query sequence. Five dene clusters with similar co-located gene arrangement and identity (threshold of 30% identity) are depicted and homologous gene sequences are shown in the same color code (Fig. S1†).

least three regulatory genes (*mdk*R, *mdk*R1, *mdk*R2).[11] While *mdk*R was annotated as TetR/AcrR-type regulator and is presumably involved in the regulation of antibiotic resistance,[21,22] *mdk*R1 is likely a member of the MerR family of regulators, known for similar functions. On the other hand, *mdk*R2 belongs to the OmpR family of response regulators, featuring a conserved receiver domain and a DNA binding motif. Prior PCR-based studies indicated that two regulators, *mdk*R1 and *mdk*R2,[23] control the gene expression of the cluster.

A functional and evolutionary analysis of the *mdk* cluster sequence by a combination of cblaster[13] and clinker[14] tool, showed that the BGC was nearly identically organized to a cluster encoded within the genome of the closely related strain *A. rayongensis* DSM 102126.[5] In contrast, the *alp* cluster in *Streptomyces ambofaciens*,[23] which encodes the biosynthesis of the structurally very closely related angucycline kinamycin, contained only a smaller core set of similar genes, and an only partial similar gene organization (Fig. 2 and S1†). Gene clusters coding for the biosynthesis of structurally related angucycline natural products, such as jadomycin (jad),[24,25] landomycin (lan),[26] and simocyclinone (sim) respectively,[27] exhibited only moderate overall similarities and different gene organizations (Fig. S4†).

Intriguingly, all analysed angucycline clusters encoded a similar domain organization of the encoded PKS, several monooxygenases and a set of regulators and transporters. However, only *mdk* encoded the halogenase *mdk*H, which was otherwise absent in related clusters. A phylogenetic analysis of the chain length factor (MdkB) and the keto synthase (MdkA) of *mdk* using the Natural product domain seeker 2[28] revealed that both share a close phylogenetic relationship to the ketosynthase of fluostatin biosynthesis (fls/fluo)[29] and the chain length factor of azicemycin biosynthesis (azicB),[30] respectively, both of which belong to the compound family angucyclines (Fig. S2–S4†).

We also noted that only one other, distantly related cluster encoded two (*mdk*R and *mdk*R1) of the three *mdk* regulators. Several of the *mdk*-related BGCs, in particular those of

Streptomyces origin, lacked sequences related to *mdk*R and *mdk*R1,[31] and harboured instead an ORF coding for an AfsA homologue, a protein essential for the biosynthesis of the auto regulatory γ-butyrolactones. Homologous sequences of *mdk*R2 were only found in every distantly related cluster, such as *chaI*, which encodes a positive regulator for angucycline production in *Streptomyces chattanoogensis*.[32] Overall, the differences in the encoded regulatory elements pinpointed towards a species-specific transcriptional regulation of the pathways causing us to hypothesize that the biosynthesized metabolites could serve as species-specific signals fulfilling external or internal signalling functions.

To test more broadly the effect of the inducing cultivation conditions, we performed a differential expression analysis of the *mdk* gene cluster. For this, *A. rubteroloni* was first cultivated for seven days under "producing" (ISP5*) and "non-producing" (ISP2) conditions (Tables S1 and S2†), and RNA was isolated from vegetative mycelium.[11] Differential expression analysis uncovered that transcript levels of *mdk*C, *mdk*E, *mdk*I (PKS) as well as *mdk*G (oxidase), *mdk*O2 (FAD-depended monooxygenase), and *mdk*H (halogenase) were higher under producing conditions compared to the levels detected for non-producing conditions (Fig. 3).

Transcripts related to precursor supply and regeneration of cofactors (*mdk*N (acyl-CoA carboxylase), *mdk*O3 (NADH-dependent reductase))[33] were likewise differentially expressed. Furthermore, transcript levels of genes encoding two putative transporter proteins (*mdk*T and *mdk*T1) and the elusive *mdk*X protein (37% similarity to *jad*X, up to 60% to other *jad*X-like genes) were increased.[34]

3.2 Heterologous expression

To verify that the *mdk* cluster is indeed responsible for the biosynthesis of angucycline natural products, the *mdk* region (see Fig. 2) was obtained from genomic DNA using a CRISPR-Cas based excision system, and then cloned into an integrative *Streptomyces* BAC (pDualp) vector. The pDualp vector
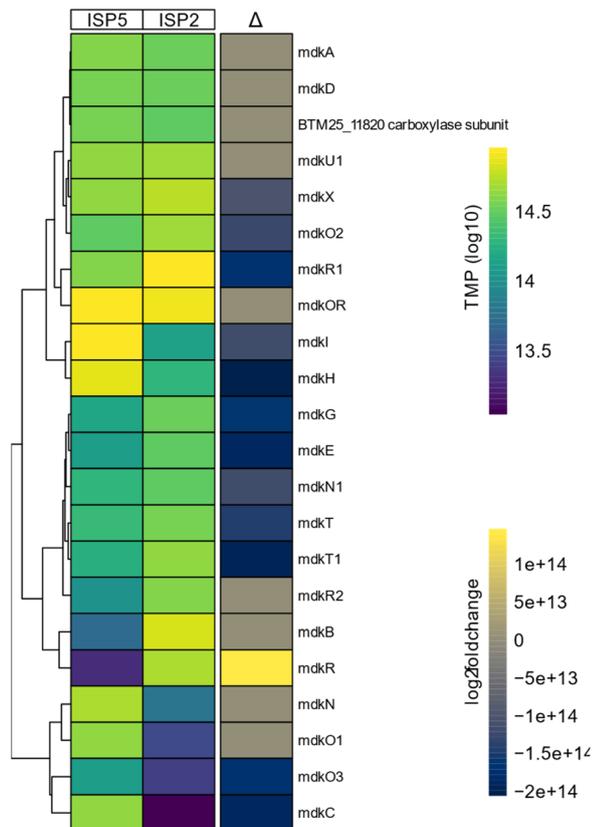
Fig. 3 Transcriptomic analysis of *A. rubteroloni* genes within the *mdk* biosynthetic gene cluster region in dependence of growth conditions (ISP2, ISP5). Heatmap of the most variable transcripts of key genes within the boundaries of the BGC *mdk* cluster. Transcript counts are shown as $\log_{10}$ transformed transcripts per million (TMP) and changes depicted as log 2 fold changes.

carried two inducible promoters, PnitA[35] and Potr,[36] which allowed induction of transcription in both reading frames in the presence of either ε-caprolactam or oxytetracycline. The vector containing the *mdk* gene cluster was then transferred into *Streptomyces albus* J1074, *Streptomyces coelicolor* M1146 and *Streptomyces lividans* TK24 as heterologous hosts by intergeneric conjugation, which was verified *via* PCR (Fig. S5–S8†). Subsequently, the cluster was heterologously expressed in all three strains (*S. albus* J1074/SAS116 α, *S. coelicolor* M1146/1.8PI; *S. lividans* TK24/1.32PISL) and the induced metabolome analyzed. The metabolome of cultures supernatants retrieved from unmodified strains *S. albus* J1074, *S. coelicolor* M1146 and *S. lividans* TK24 served as control samples. As the presence of the inducer oxytetracycline caused reduced biomass formation of *S. albus* J1074 and the modified strain SAS116α, both strains were also cultivated in DNPM broth containing only ε-caprolactam. For metabolomic analysis, supernatants of induced cultures were concentrated using a standardized solid-phase extraction (SPE) procedure and subsequently analyzed by liquid-chromatography coupled with tandem mass spectrometry (LC-HRMS/MS). Comparative analysis of culture extracts showed that modified strains (J1074, 1.8PI, 1.32PISL) exhibited

an upregulation of known host-specific metabolites in all experiments.

Only strain *S. albus* J1074/SAS116 α[37] was found to produce one additional ε-caprolactam-induced metabolite compared to the controls, which correlated to a distinct UV peak at 7.61 min (λ_{max} at 285 and 511 nm, $[M + H]^+ = 454.0947$) and thus was sought to be likely responsible for the greenish color of the culture (Fig. 4). We also performed an extensive targeted metabolomic survey of *m/z* features that correlated to $[M + H]^+$ values of maduralactomycins/actinospirols and derivatives thereof; however, neither the exact *m/z* values nor related molecular ion peaks were detected (Fig. S9–S19†).

To test if regulators MdkR and MdkR1 are involved in the transcriptional regulation of the *mdk* pathway, we employed a knock-out strategy using the λ red system, in which a resistance marker replaces the respective gene *via* homologous recombination in *E. coli*.[38] Using this technique, *mdk*R and *mdk*R1 were replaced with a spectinomycin resistance cassette yielding the plasmid ΔacrR. The edited plasmid was then transferred to the heterologous host *S. albus* J1074/SAS116 α *via* conjugation yielding strain SaΔacrR (Fig. S5–S8†). Subsequent heterologous expression experiments were performed using the mutated *S. albus* J1074/SaΔacrR, strain SAS116α carrying the unedited plasmid, and the wild type *S. albus* J1074 (control). Metabolites of culture supernatants were enriched by SPE extraction and subjected to LC-MS/MS-analysis. Manual targeted searches and network-based analysis of MS-datasets for *mdk*-related angucyclic metabolite products (Fig. S15–S19 and Tables S6–S8†) revealed several shared secondary metabolite related clusters, including the host-specific natural product family surugamides.[39] Only one molecular ion cluster was unique to *S. albus* J1074/SAS116 α, which contained three connected nodes with related molecular ions features (*m/z* 454.095, 452.079, 468.074), and were otherwise absent in culture extracts of the deletion mutant strain SaΔacrR and *S. albus* J1074. To elucidate the structure of the induced metabolite, strain SAS 116α was cultivated and metabolites of the culture supernatant enriched using our standard C_{18}-based SPE protocol. The resulting 10% and 30% MeOH/H$_2$O eluents were subjected to
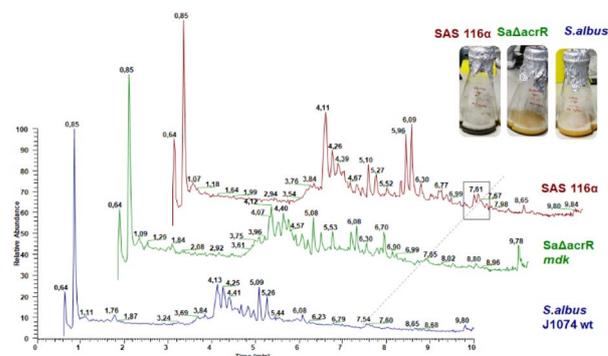

Fig. 4 Total ion chromatogram (TIC) of SAS116 α, SaΔacrR and *S. albus* J1074 with SAS116 α showing production of seongomycin (7.61 min) as well as the upregulated production of several wild type-derived natural product families.
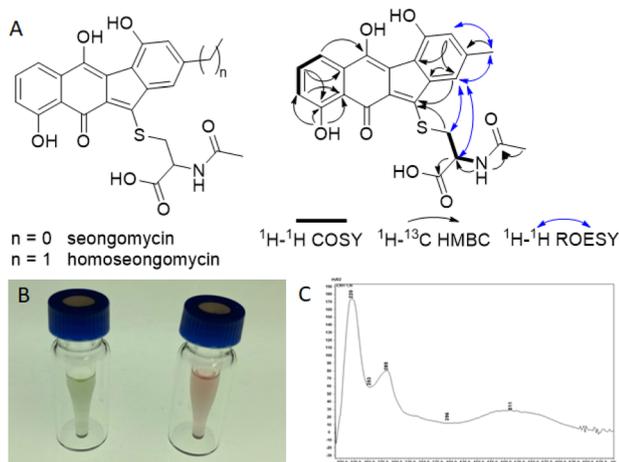
Fig. 5 (A) Chemical structure of seongomycin and homo-seongomycin and key 2D NMR correlations for seongomycin; (B) solution of seongomycin in methanol (green) and in the presence of approx. 1% formic acid (red); (C) UV absorption spectrum of seongomycin (MeOH).
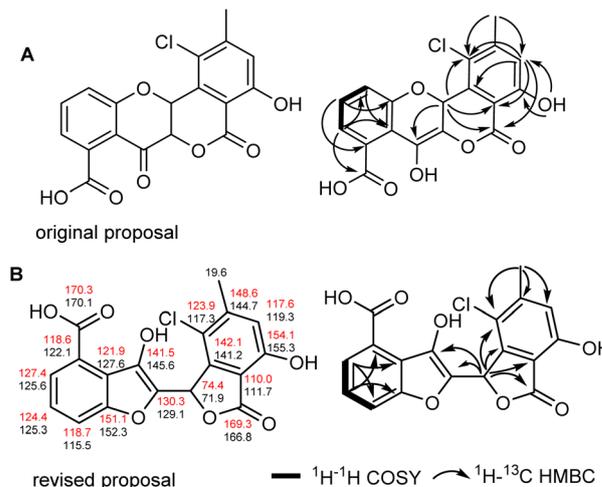

Fig. 6 (A) Original proposed structure of maduralactomycin A and key 2D NMR correlations for original proposed structure; (B) revised chemical structure of maduralactomycin A with ^{13}C-chemical shifts (calculated: red; experimental: black) and key 2D NMR correlations for revised structure proposal.

a UV-Vis- and MS-guided protocol using semi-preparative HPLC, yielding 9.24 mg of the major product (m/z 454.095, approx. production titer: 23 mg L^{-1}) together with minor amounts of an analog ($m/z = 468.074$, $m/z = 14$ Da) (Fig. S20 and S21†). During the work-up, we also noted a pH-depended UV-absorption related to the produced compound, which was visible in a reversible color shift of the product in solution and solid state. Comparative 1D and 2D NMR analysis of the major isolated compound ([M + H]$^+$ = 454.0947) uncovered matching ^{1}H and ^{13}C chemical shifts (d_6-DMSO + 1% d$_1$-TFA) with the previously reported angucyclic metabolite seongomycin (Fig. 5, S22–S32 and Table S9†) and those obtained by computational NMR analysis (Table S10†). The minor metabolite was identified as homoseongomycin based on matching HRMS/MS data and comparison of chemical shift values (Fig. S22 and S23).[11,40]

3.3 Structural revision of maduralactomycin A

The formation of seongomycin, which shows a different regio-chemical orientation of the substituents in ring A compared to maduralactomycin A (Fig. 6A), stimulated us to revisit the analytical datasets of the previously isolated maduralactomycin A and the proposed biosynthetic pathway, which remained ambiguous despite extensive ^{13}C-labeling and computation efforts (Table S11†).

Using of a combination of geometry optimization of determined conformers based on B3LYP/6-31+G(d,p) level of theory in the gas-phase, we re-calculated the ^{13}C and ^{1}H chemical shifts values of twenty-six regioisomers (Fig. S33 and Tables S12–S17†). Shielding tensors were then computed at mPW1PW91/6-311+G(2d,p) level of theory with polarizable continuum model (PCM).[41] Extensive comparative NMR analysis allowed us to identify two chemical structures, which showed the best matching chemical shift pattern and correlations of which only one fitted the observed ^{13}C-labling pattern, (Fig. S34 and Tables S19–S21†). Hence, we propose here

a revised structure of maduralactomycin A (Fig. 6B), which now is composed of two benzofuranone-like moieties inter-connected by C–C bond and carries expected actinospirol-like substitution pattern (methylation, chlorination).

3.4 Biosynthetic reconsiderations

The successful expression of the *mdk* cluster in *S. albus* J1074 as heterologous host confirmed the angucyclic nature of the *mdk* cluster products. The angucyclic product seongomycin contains a ring system akin to the modified structure of madur-alactomycin A, featuring a contracted 6,5,5,6 ring arrangement. However, a notable distinction lies in the linkage of the two five-membered ring systems, attributed to the presence of an extra bridging carbon atom (presumably C-14). Further structural disparities encompass the changed position of the methyl and hydroxyl groups within the A-ring and the absence of the halogenation pattern. Consequently, we postulate that seongo-mycin is likely a by- or shuntproduct of the heterologously expressed *mdk* pathway. To trace the origin of seongomycin, we then re-analyzed the biosynthetic proposal (Fig. 7). The initial step of the biosynthesis includes a typical type II polyketide pathway, in which the synthase utilizes an acetyl-CoA starter unit and malonyl-CoA extender units to generate a highly reactive acyl-carrier protein (ACP)-bound poly-β-ketone chain (I, Fig. 7). The next biosynthetic step in the biosynthesis involves the didomain polyketide cyclase MdkD, which should initiate the cyclization cascade of poly-β-ketone chain to yield the aromatized intermediate II.[42]

The sequence of oxygenation, oxidative ring cleavage and ring contraction, which is accompanied by the loss of C-1 and C-15, is likely catalyzed by the ring opening oxygenase MdkG (AlpJ)[43] MdkO1, MdkO2 and MdkOR should yield the precursor kinobscurinone as previously reported. Chlorination is proposed to be catalyzed by MdkH at an early stage of the
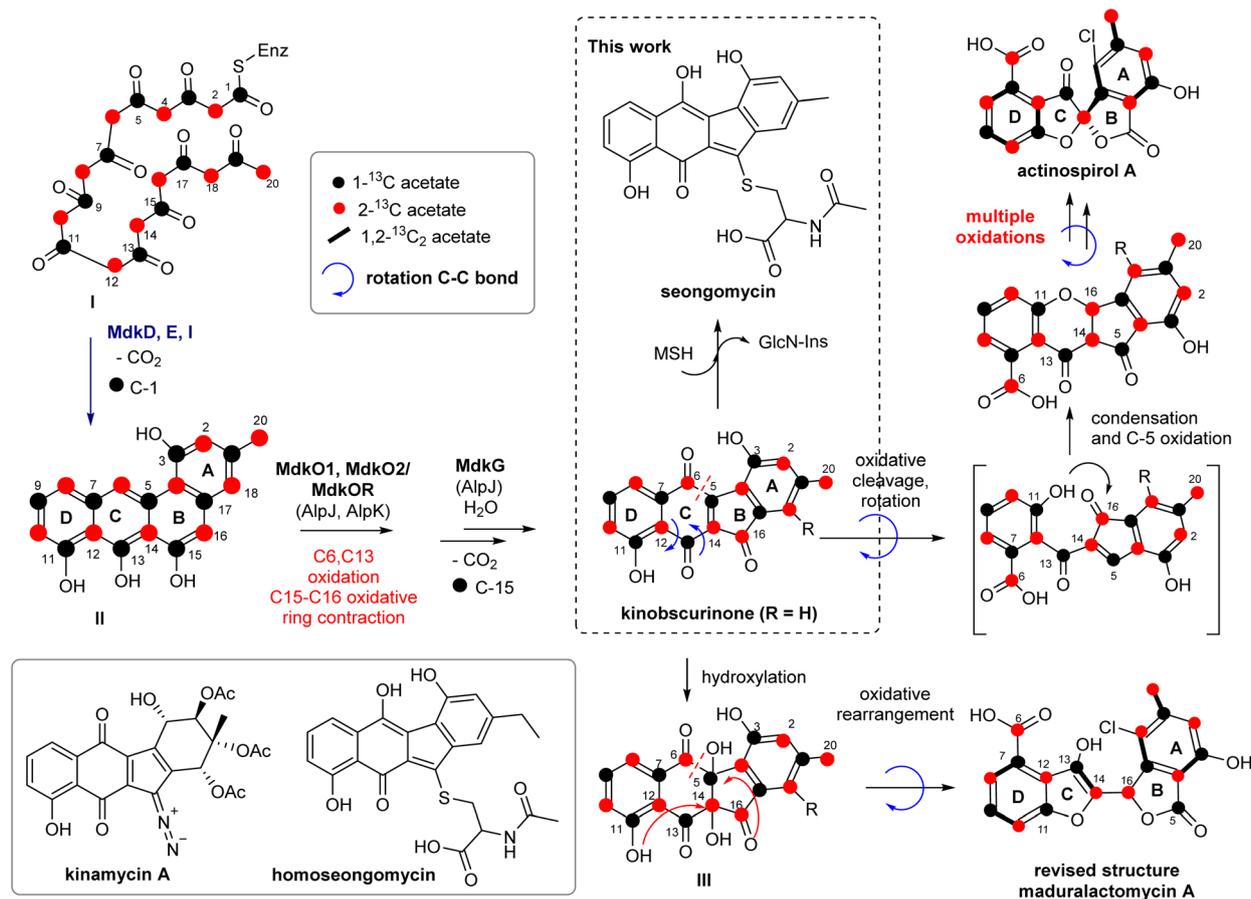
Fig. 7 Reconsideration of putative key transformations involved in the biosynthesis of (A) seongomycin and (B) structurally revised madur‐alactomycin A based on prior ^{13}C-labeling and gene cluster analysis (Fig. S33 and Tables S18–S20†).

biosynthesis as only one position in both natural products was regioselectively halogenated. As neither chlorination of seon‐gomycin nor putative biosynthetic precursors were observed within this study, we hypothesize that MdkH is either highly substrate specific or dysfunctional due to the heterologous expression in *S. albus* J1074 SAS 116α.

The formation of seongomycin, however, also highlights the limitation of *S. albus* as heterologous host as the AcCys S‐conjugate likely represents a mycothiol-based detoxification product of kinobscurinone. The formation of seongomycin can be reasoned as follows: (1) nucleophilic addition of mycothiol (MSH), a protective agent found in Gram-positive *Streptomycetes* that safeguards cells against toxic and reactive electrophiles, to the intermediate kinobscurinone; (2) subsequent water elimi‐nation, double bond isomerization, and a reduction; and (3) cleavage of the MSH-conjugate by a specific amidase, resulting in the release of GlcN-Ins (1-D-myo-inosytyl 2-amido-2-deoxy-α-D-glucopyranoside) and the AcCys S-adduct.[44,45] Hence, it can be inferred that when aiming for the heterologous production of natural products formed from reactive intermediates suscep‐tible to 1,4-Michael additions or acetal formation, heterologous hosts known for generating elevated quantities of MSH should be avoided.

3.5 Bioactivities

We also evaluated the pharmacological profile of seongomycin more in detail and performed antibacterial, antifungal, antiviral and cytological tests (Tables S22–S25 and Fig. S34–S37†). However, neither antimicrobial activity nor an antiproliferative effect on the HeLa cell lines was detectable. Although a recent antiviral assay of homoseongomycin, a close derivative of seongomycin, revealed activity of this compound against certain species of alpha viruses,[46] seongomycin showed neither antiviral effects against the coronaviruses (SARS-CoV-2, HCoV-229E), Respiratory Syncytial Virus (RSV) nor the human patho‐genic alpha virus Chikungunya-Virus (CHIKV).

4. Conclusions

In this study, we successfully expressed the *mdk* cluster in *S. albus* J1074/SAS116 α, leading to the biosynthesis of the angu‐cyclic product seongomycin. Notably, heterologous production was effectively abolished upon the knockout of two pivotal regulators within the pathways. Additionally, we accomplished a revision of the core structure of maduralactomycin through a computational approach combined with 2D NMR analysis. The work presented herein establishes the chemical and

molecular biological groundwork for systematic investigations of the *mdk* pathway across diverse host systems. It furthermore enables pathway manipulation to identify key biosynthetic intermediates and unravel the nature of the distinctive oxidative biosynthetic rearrangement steps.

Author contributions

JWS contributed to conceptualization, data curation, writing – original draft, review and editing. HL, SU, FS contributed by formal analysis, investigation, validation and visualization as well as formal analysis. MBrö, MBau, CB contributed with conceptualization, formal analysis, funding acquisition, supervision, validation, visualization, writing – original draft, review and editing.

Conflicts of interest

There are no conflicts to declare.

Acknowledgements

Notes and references

1 E. B. Van Arnam, C. R. Currie and J. Clardy, *Chem. Soc. Rev.*, 2018, **47**, 1638–1651.

2 M. Miethke, M. Pieroni, T. Weber, M. Brönstrup, P. Hammann, L. Halby, P. B. Arimondo, P. Glaser, B. Aigle, H. B. Bode, R. Moreira, Y. Li, A. Luzhetskyy, M. H. Medema, J. L. Pernodet, M. Stadler, J. R. Tormo, O. Genilloud, A. W. Truman, K. J. Weissman, E. Takano, S. Sabatini, E. Stegmann, H. Brötz-Oesterhelt, W. Wohlleben, M. Seemann, M. Empting, A. K. H. Hirsch, B. Loretz, C. M. Lehr, A. Titz, J. Herrmann, T. Jaeger, S. Alt, T. Hesterkamp, M. Winterhalter, A. Schiefer, K. Pfarr, A. Hoerauf, H. Graz, M. Graz, M. Lindvall, S. Ramurthy, A. Karlén, M. van Dongen, H. Petkovic, A. Keller, F. Peyrane, S. Donadio, L. Fraisse, L. J. V. Piddock, I. H. Gilbert, H. E. Moser and R. Müller, *Nat. Rev. Chem*, 2021, **5**, 726–749.

3 D. A. van Bergeijk, B. R. Terlouw, M. H. Medema and G. P. van Wezel, *Nat. Rev. Microbiol.*, 2020, **18**, 546–558.

4 M. J. Smanski, D. C. Schlatter and L. L. Kinkel, *J. Ind. Microbiol. Biotechnol.*, 2016, **43**, 115–128.

5 R. Benndorf, K. Martin, M. Küfner, Z. W. de Beer, J. Vollmers, A.-K. Kaster and C. Beemelmanns, *Int. J. Syst. Evol. Microbiol.*, 2020, **70**, 5255–5262.

6 R. Benndorf, H. Guo, E. Sommerwerk, C. Weigel, M. Garcia-Altares, K. Martin, H. Hu, M. Kuefner, Z. W. de Beer, M. Poulsen and C. Beemelmanns, *Antibiotics*, 2018, **7**, E83.

7 H. Guo, R. Benndorf, D. Leichnitz, J. K. Klassen, J. Vollmers, H. Görls, M. Steinacker, C. Weigel, H. M. Dahse, A. K. Kaster, Z. W. de Beer, M. Poulsen and C. Beemelmanns, *Chem. – Eur. J.*, 2017, **23**, 9338–9345.

8 H. Guo, R. Benndorf, S. König, D. Leichnitz, C. Weigel, G. Peschel, P. Berthel, M. Kaiser, C. Steinbeck, O. Werz, M. Poulsen and C. Beemelmanns, *Chem. – Eur. J.*, 2018, **24**, 11319–11324.

9 Y. Yan, J. Yang, Z. Yu, M. Yu, Y. Ma, L. Wang, C. Su, J. Luo, G. P. Horsman and S. Huang, *Nat. Commun.*, 2016, **7**, 13083.

10 X. Cai, Y.-M. Shi, N. Pöhlmann, O. Revermann, I. Bahner, S. J. Pidot, F. Wesche, H. Lackner, C. Büchel, M. Kaiser, C. Richter, H. Schwalbe, T. P. Stinear, A. Zeeck and H. B. Bode, *Angew. Chem., Int. Ed.*, 2017, **56**, 4945.

11 H. Guo, J. W. Schwitalla, R. Benndorf, M. Baunach, C. Steinbeck, H. Görls, Z. W. de Beer, L. Regestein and C. Beemelmanns, *Org. Lett.*, 2020, **22**, 2634–2638.

12 K. Blin, S. Shaw, A. M. Kloosterman, Z. Charlop-Powers, G. P. van Weezel, M. H. Medema and T. Weber, *Nucleic Acids Res.*, 2021, **49**, W29–W35.

13 C. L. M. Gilchrist, T. J. Booth, B. van Wersch, L. van Grieken, M. H. Medema and Y.-H. Chooi, *Bioinf. Adv.*, 2021, **1**, vbab016.

14 C. L. M. Gilchrist and Y.-H. Chooi, *Bioinformatics*, 2021, **37**, 2473–2475.

15 T. Kieser, M. J. Bibb, M. J. Buttner, K. F. Chater and D. A. Hopwood, *Practical Streptomyces genetics*, John Innes Foundation Norwich, 2000, vol. 291.

16 B. Gust, T. Kieser and K. Chater, *PCR targeting system in Streptomyces coelicolor A3 (2)*, John Innes Centre, 2002, vol. 3, 2, pp. 1–39.

17 M. Wang, J. J. Carver, V. V. Phelan, L. M. Sanchez, N. Garg, Y. Peng, D. D. Nguyen, J. Watrous, C. A. Kapono, T. Luzzatto-Knaan, C. Porto, A. Bouslimani, A. V. Melnik, M. J. Meehan, W. T. Liu, M. Crüsemann, P. D. Boudreau, E. Esquenazi, M. Sandoval-Calderón, R. D. Kersten, L. A. Pace, R. A. Quinn, K. R. Duncan, C. C. Hsu, D. J. Floros, R. G. Gavilan, K. Kleigrewe, T. Northen, R. J. Dutton, D. Parrot, E. E. Carlson, B. Aigle, C. F. Michelsen, L. Jelsbak, C. Sohlenkamp, P. Pevzner, A. Edlund, J. McLean, J. Piel, B. T. Murphy, L. Gerwick, C. C. Liaw, Y. L. Yang, H. U. Humpf, M. Maansson, R. A. Keyzers, A. C. Sims, A. R. Johnson, A. M. Sidebottom, B. E. Sedio, A. Klitgaard, C. B. Larson, C. A. P. Boya, D. Torres-Mendoza, D. J. Gonzalez, D. B. Silva, L. M. Marques, D. P. Demarque, E. Pociute, E. C. O'Neill, E. Briand, E. J. N. Helfrich, E. A. Granatosky, E. Glukhov, F. Ryffel, H. Houson, H. Mohimani, J. J. Kharbush, Y. Zeng, J. A. Vorholt, K. L. Kurita, P. Charusanti, K. L. McPhail, K. F. Nielsen, L. Vuong, M. Elfeki, M. F. Traxler, N. Engene, N. Koyama, O. B. Vining,

R. Baric, R. R. Silva, S. J. Mascuch, S. Tomasi, S. Jenkins, V. Macherla, T. Hoffman, V. Agarwal, P. G. Williams, J. Dai, R. Neupane, J. Gurr, A. M. C. Rodríguez, A. Lamsa, C. Zhang, K. Dorrestein, B. M. Duggan, J. Almaliti, P. M. Allard, P. Phapale, L. F. Nothias, T. Alexandrov, M. Litaudon, J. L. Wolfender, J. E. Kyle, T. O. Metz, T. Peryea, D. T. Nguyen, D. VanLeer, P. Shinn, A. Jadhav, R. Müller, K. M. Waters, W. Shi, X. Liu, L. Zhang, R. Knight, P. R. Jensen, B. Palsson, K. Pogliano, R. G. Linington, M. Gutiérrez, N. P. Lopes, W. H. Gerwick, B. S. Moore, P. C. Dorrestein and N. Bandeira, *Nat. Biotechnol.*, 2016, **34**, 828–837.

18 D. Petras, V. V. Phelan, D. Acharya, A. E. Allen, A. T. Aron, N. Bandeira, B. P. Bowen, D. Belle-Oudry, S. Boecker, D. A. Jr Cummings, J. M. Deutsch, E. Fahy, N. Garg, R. Gregor, J. Handelsman, M. Navarro-Hoyos, A. K. Jarmusch, S. A. Jarmusch, K. Louie, K. N. Maloney, M. T. Marty, M. M. Meijler, I. Mizrahi, R. L. Neve, T. R. Northen, C. Molina-Santiago, M. Panitchpakdi, B. Pullman, A. W. Puri, R. Schmid, S. Subramaniam, M. Thukral, F. Vasquez-Castro, P. C. Dorrestein and M. Wang, *Nat. Methods*, 2022, **19**, 134–136.

19 N. T. H. Le, T. Vermeyen, R. Aerts, W. A. Herrebout, L. Pieters and E. Tuenter, *Molecules*, 2023, **28**, 214.

20 N. T. H. Le, E. Van Roy, E. Dendooven, L. Peeters, M. Theunis, K. Foubert, L. Pieters and E. Tuenter, *Phytochemistry*, 2021, **190**, 112863.

21 I. Ostash, B. Ostash, A. Luzhetskyy, A. Bechthold, S. Walker and V. Fedorenko, *FEMS Microbiol. Lett.*, 2008, **285**, 195–202.

22 L. Cuthbertson and J. R. Nodwell, *Microbiol. Mol. Biol. Rev.*, 2013, **77**, 440–475.

23 R. Bunet, L. Song, M. V. Mendes, C. Corre, L. Hotel, N. Rouhier, X. Framboisier, P. Leblond, G. L. Challis and B. Aigle, *J. Bacteriol.*, 2011, **193**, 1142–1153.

24 K. Kulowski, E. W. Pienkowski, L. Han, K. Q. Yang, L. C. Vining and C. R. Hutchinson, *J. Am. Chem. Soc.*, 1999, **121**, 1786–1794.

25 Y. H. Chen, C. C. Wang, L. Greenwell, U. Rix, D. Hoffmeister, L. C. Vining, J. Rohr and K. Q. Yang, *J. Biol. Chem.*, 2005, **280**, 22508–22514.

26 P. Patrikainen, P. Kallio, K. Fan, K. D. Klika, K. A. Shaaban, P. Mäntsälä, J. Rohr, K. Yang, J. Niemi and M. Metsä-Ketelä, *Chem. Biol.*, 2012, **19**, 647–655.

27 A. Trefzer, S. Pelzer, J. Schimana, S. Stockert, C. Bihlmaier, H. P. Fiedler, K. Welzel, A. Vente and A. Bechthold, *Antimicrob. Agents Chemother.*, 2002, **46**, 1174–1182.

28 L. J. Klau, S. Podell, K. E. Creamer, A. M. Demko, H. W. Singh, E. E. Allen, B. S. Moore, N. Ziemert, A. C. Letzel and P. R. Jensen, *J. Biol. Chem.*, 2022, **298**, 102480.

29 Z. Feng, J. H. Kim and S. F. Brady, *J. Am. Chem. Soc.*, 2010, **132**, 11902–11903.

30 Y. Ogasawara and H.-W. Liu, *J. Am. Chem. Soc.*, 2009, **131**, 18066–18068.

31 J. y. Kato, N. Funa, H. Watanabe, Y. Ohnishi and S. Horinouchi, *Proc. Natl. Acad. Sci. U. S. A.*, 2007, **104**, 2378–2383.

32 Z. Zhou, Q. Xu, Q. Bu, Y. Guo, S. Liu, Y. Liu, Y. Du and Y. Li, *ChemBioChem*, 2015, **16**, 496–502.

33 V. Blanc, D. Lagneaux, P. Didier, P. Gil, P. Lacroix and J. Crouzet, *J. Bacteriol.*, 1995, **177**, 5206–5214.

34 A. W. Robertson, S. M. Forget, C. F. Martinez-Farina, N. E. McCormick, R. T. Syvitski and D. L. Jakeman, *J. Am. Chem. Soc.*, 2016, **138**, 2200–2208.

35 M. Matsumoto, Y. Hashimoto, Y. Saitoh, T. Kumano and M. Kobayashi, *Biosci., Biotechnol., Biochem.*, 2016, **80**, 1230–1237.

36 W. Wang, T. Yang, Y. Li, S. Li, S. Yin, K. Styles, C. Corre and K. Yang, *ACS Synth. Biol.*, 2016, **5**, 765–773.

37 M. Myronovskyi and A. Luzhetskyy, *Nat. Prod. Rep.*, 2019, **36**, 1281–1294.

38 B. Gust, G. L. Challis, K. Fowler, T. Kieser and K. F. Chater, *Proc. Natl. Acad. Sci. U.S.A.*, 2003, **100**, 1541–1546.

39 F. Xu, B. Nazari, K. Moon, L. B. Bushin and M. R. Seyedsayamdost, *J. Am. Chem. Soc.*, 2017, **139**, 9203–9212.

40 C. M. Woo, S. L. Gholap and S. B. Herzon, *J. Nat. Prod.*, 2013, **76**, 1238–1241.

41 H. T. N. Le, E. Van Roy, E. Dendooven, L. Peeters, M. Theunis, K. Foubert, L. Pieters and E. Tuenter, *Phytochemistry*, 2021, **190**, 112863.

42 S.-C. Tsai, *Annu. Rev. Biochem.*, 2018, **87**, 503–531.

43 S. Lösgen, Ö. Schlörke, K. Meindl, R. Herbst-Irmer and A. Zeeck, *Eur. J. Org Chem.*, 2007, **13**, 2191–2196.

44 G. Newton and R. Fahey, *Arch. Microbiol.*, 2002, **178**, 388–394.

45 V. K. Jothivasan and C. J. Hamilton, *Nat. Prod. Rep.*, 2008, **25**, 1091–1117.

46 S. C. Lin, C. W. Lehman, A. K. Stewart, L. Panny, N. Bracci, J. L. C. Wright, M. Paige, W. K. Strangman and K. Kehn-Hall, *Antiviral Res.*, 2021, **191**, 105087.